ЄE

UR-1340
ER-40685-789



# ELECTRON EMISSION FROM METALLIC SURFACES BY PICOSECOND LASER PULSES

Alan R. Fry and A. C. Melissinos
Department of Physics and Astronomy
University of Rochester
Rochester, NY 14627

1/94

UNIVERSITY OF ROCHESTER

DEPARTMENT OF PHYSICS AND ASTRONOMY

ROCHESTER, NEW YORK 14627

UR-1340
ER-40685-789
January 1994

# ELECTRON EMISSION FROM METALLIC SURFACES BY PICOSECOND LASER PULSES

Alan R. Fry and A. C. Melissinos
Department of Physics and Astronomy
University of Rochester
Rochester, NY 14627

## Abstract

We have measured the photoemission yields from metallic surfaces using picosecond laser pulses. We plan to use photoemission as an electron source in a compact superconducting laser-driven electron gun. By backscattering the laser pulse from the electron beam, a time resolved, quasi-coherent X-ray beam is produced.

## 1. Motivation

In many recent applications it is desirable to have short, intense electron pulses with good emittance. Such beams can be effectively produced with "r.f. guns". In these devices an electron source is placed in an accelerating microwave (r.f.) cavity and the emitted electrons are accelerated directly by the r.f. field without preacceleration by a D.C. voltage and subsequent bunching. Furthermore, in an r.f. gun, electron emission can be conveniently achieved by a short laser pulse. Laser r.f. guns result in smaller transverse momenta of the electron beam because of the cold cathode, and produce large electron current densities at the cathode. Laser excitation is also important in producing polarized electron beams.

Because the electrons must be accelerated from rest to relativistic velocities within one half r.f. cycle, laser r.f. guns require high electric fields and thus high power input. This is achieved by pulsed operation at the megawatt level. An alternative is the use of a superconducting r.f. cavity where the same field can be established at much lower power levels, and the cavity can operate continuously.

In this application it seems desirable – at least in the initial stages – to photoemit the electrons directly from the Niobium surface of the cavity. The laser power must be restricted so as not to drive the cavity normal. We have therefore studied photoemission from Nb, Cu and Au surfaces using a UV laser pulse of ~20 ps duration with total energy in the pulse between 10-100 $\mu$J.

## 2. Experimental Arrangement

The laser pulses were obtained from a "chirped" laser amplification system consisting of a YLF oscillator and glass regenerative amplifier[1], operating at 1 Hz. The wavelength was $\lambda = 1054$ nm, and we used the entire pulse train from the amplifier rather than selecting a single pulse; the pulses were compressed in time to approximately 20 ps duration. The IR pulses were then frequency doubled to green and doubled again to UV using BBO crystals, to produce a final wavelength of $\lambda = 264$ nm. The energy in the IR pulse train was of order of few mJ resulting in 10-100 $\mu$J in the UV. Typically the UV pulse train contained about 8 pulses as shown in Fig.1. The UV energy was monitored for every pulse by sending a fraction of the pulse to a power meter.

The metallic cathodes were flat discs, 1-inch in diameter mounted on an electrically isolated holder which was connected to ground through a charge-sensitive amplifier (Amptek A-225). The anode, a metallic disc with a 2 mm diameter hole to let the laser pulse pass through it to the cathode, was biased to a variable positive voltage up to 3 kV; in previous experiments the anode was a metallic mesh. We also took data with the cathode illuminated at almost tangential incidence. In this case the polarization of the light pulse was varied with respect to the plane of incidence. The experimental arrangement is shown schematically in Fig.2. A turbo pump was used to maintain a vacuum in the $10^{-8}$ torr range.

The integrated charge as measured by the amplifier and the laser pulse intensity were digitized on a Tektronix, TDS-620 scope for each pulse. These data were accumulated and displayed on a Macintosh IIci using National Instruments Labview. Typically 100 pulses were averaged at each setting and their error was calculated from the dispersion of the results. The principal cause for such dispersion are the fluctuations in the laser intensity. The integrator was calibrated by injecting a known charge, and its dynamic range could be adjusted from 0.1 to 40 pC.

The cleanliness and preparation of the cathodes appears to be of crucial importance in determining the quantum efficiency. The Nb and Cu cathodes were mechanically polished and then cleaned with an acid solution. The gold cathode was made by evaporating an 88:12 mixture of Au and Ge on a Cu substrate to an estimated thickness of 100 nm. It gave the highest efficiency so far (see Fig.6(b)) We also tried other cathodes, such as $LaB_6$ deposited on a sapphire disc but the results were inconclusive.

## 3. Results

The data are presented as the ratio of charge collected (in pC) to UV incident on the cathode (in $\mu$J). Corrections for light losses at windows and other optics have been made. The quantum efficiency (electrons/photon) can be obtained by multiplying the pC/$\mu$J ratio by the photon energy in eV $\times 10^{-6}$. Thus

$$\epsilon = \left(\frac{pC}{\mu J}\right) \times 4.70 \times 10^{-6} \tag{1}$$

We first present the Nb data in some detail. We obtained normal incidence data at two different spacings of the anode from the cathode. The laser pulse was of circular cross section with a 2 mm diameter, and the pulse length is estimated at $\tau = 20$ ps per pulse in the train. The data are shown as a function of bias voltage and for different UV energies in Fig.3(a) for the 5 mm spacing and in Fig.3(b) for the 1.1 mm spacing. In both cases the increase in yield is much more gradual than the space-charge limited $V^{3/2}$ dependence. Furthermore the yield for the five-fold higher field of the 1.1 mm spacing is not significantly larger than for the 5 mm gap. We conclude that we are emission limited and not space charge limited.

The best efficiency observed from these data is of order $\epsilon = 10^{-6}$. The corresponding peak current density (at 100 $\mu$J) is

$$J = \frac{\Delta Q}{\tau}\frac{1}{A} = 1.5 \quad \mathrm{A/cm^2} \tag{2}$$

where we approximated $\Delta Q = Q/8$ to account for the multiple pulses in the train. For a planar diode with 5 mm gap and at 2.5 kV bias the space-charge limited current density is

$$J = \frac{2.34 \times 10^{-6}[V(\mathrm{Volts})]^{3/2}}{[d(\mathrm{cm})]^2} \quad (\mathrm{A/cm^2}) = 1.2 \quad \mathrm{A/cm^2} \tag{3}$$

The corresponding intensity of the laser pulse is estimated to be

$$I = \frac{\Delta E}{\tau} \frac{1}{A} \sim 9 \ \ \mathrm{MW/cm^2}$$

where $\Delta E = E/8$ is the average energy in each pulse.

In Figs.4(a) and 4(b) the same data are presented as a function of UV energy for the different applied biases for the two gaps, 1.1 mm and 5.1 mm. The apparent small drop in efficiency is not strongly dependent on the bias, and is attributed to saturation of the charge integrator.

Data from the Nb cathode were also obtained with the beam incident at 80° with respect to the normal. The data are shown in Fig.5(a) as a function of a laser beam polarization for different UV energies; the gap was 5.1 mm and the bias 3 kV. The yield depends on the polarization and is maximum for p-polarization (E-field in the plane of incidence). The data for all UV energies are fitted with the same $\cos^2(2\phi)$ curve where $\phi$ is the angle of the half-wave plate. The combined data are shown in Fig.5(b) indicating a 14% modulation which we interpret as field-assisted emission. We performed control experiments to ascertain that the peaks correspond (within $\pm 10°$) to p-polarization and that such polarization effects are absent at normal incidence. The average efficiency in this case was $\epsilon = 0.6 \times 10^{-6}$. In contrast, in the same geometry but for a 1.1 mm gap spacing efficiencies as high as $1.6 \times 10^{-5}$ were obtained. The effective beam size for "grazing" incidence was of order 18 $\mathrm{mm}^2$ as compared to 3 $\mathrm{mm}^2$ for normal incidence; the current density was therefore correspondingly lower.

Results from Cu, Au and Nb cathodes were obtained at normal incidence in a series of previous measurements. As for the data discussed above, the cathode was connected to ground through the charge integrating amplifier. The anode was a metallic mesh with 43% transmission and biased to positive voltage; the gap between cathode and anode was 2.7 mm. Fig.6 gives the efficiency as a function of biasing field for the three cathodes. The Nb results are consistent with our present measurements but lower than those given in Figs. 3-5. No significant dependence on the bias voltage is observed. The residual pressure for the measurements shown in Fig.6(a) was as follows

| | |
|---|---|
| Au cathode | $P = 6 \times 10^{-9}$ torr |
| Cu | $3 \times 10^{-8}$ torr |
| Nb | $5 \times 10^{-8}$ torr |

How much the residual pressure affects the surface cleanliness and efficiency has not been determined at this point. Furthermore during a recent run the efficiency of another Cu cathode at grazing incidence (gap 5.1 mm) reached only $\epsilon = 0.7 \times 10^{-6}$, nearly a factor of three below the data of Fig.6(a). Recent results from a Au cathode at normal incidence are shown in Fig.6(b) as a function of applied field, for different incident UV energy.

## 4. Discussion

There is a significant variation in the literature for the reported values of the work functions of metals. For the cathode materials we have tested, we list a range of reported work functions below:

| | |
|---|---|
| Au | 4.3-5.47 eV |
| Cu | 4.4-4.94 eV |
| Nb | 4.0-4.63 eV |

to be compared to the UV photon energy $hv = 4.7$ eV. The upper limit is the highest of several values compiled by Michaelson[(2)], and the lower limit is that recommended by Fomenko from his earlier compilation[(3)]. For each material we tested, Fomenko's recommended value is lower than the lowest Michaelson values.

For low incident light intensities the photoelectron yield should vanish when the photon energy of the light is below the work function $\phi$ of the metal, i.e. for $hv < \phi$. In the work functions for Cu and Nb are consistently reported as being below 4.7 eV, particularly when measured by photoelectric emission. In every photoelectric emission study from the above references, however, the work function of Au is measured *above* 4.72 eV. That we consistently measure a significant photoelectric yield from Au may be attributed to a combination of 2-photon absorption and barrier lowering by the Schottky effect. For a 13 $MW/cm^2$ pulse the electric field in the laser reaches $E = 10^5$ V/cm; the Schottky barrier suppression is given by $\Delta\phi = [(e/4\pi\varepsilon_0)E]^{1/2}$ which corresponds to $\Delta\phi = 0.12$ V for the above field. We have not observed any photoelectric yield from Au when exposed to green light (2.35 eV) of similarly high intensity, which limits the possible contribution of multiphoton absorption.

Studies of photoemission by short laser pulses have been carried out by Fischer and Srinivasan-Rao[4], who give the quantum efficiency as

$$\epsilon = 2 \times 10^{-4}(h\nu - \phi)^2 \tag{4}$$

They used a quadrupled YAG laser ($h\nu = 4.65$ eV) and studied Au, Mg, Y, Te and Sa cathodes. Our results for Au are in agreement within a factor of two of theirs. These authors mention that their cathodes were specially prepared and their residual vacuum was in the $10^{-9}$ torr range.

Charpak et al.[5] report on photoemission from Cu and Al cathodes using c.w. UV. Their data for Cu can be fitted by

$$\epsilon = 2 \times 10^{-6}(h\nu - \phi_0)^2 \tag{5}$$

where the light source frequency is varied and $\phi_0$ is taken as 4.15 eV. The efficiency increased by two orders of magnitude when the cathodes were coated with organic substances such as TMAE. Cesiated surfaces are known to have efficiencies up to 0.1 and they photoemit with visible light. However such surfaces must be prepared in situ and introduced into the gun through a vacuum lock; $LaB_6$ is a good material for thermionic cathodes and can be used in a laser gun if warmed slightly. Neither condition is well suited for our proposed application.

In our work so far we have difficulty with the reproducibility of our results. For instance in earlier work[1] we reported efficiencies for Au at normal incidence $\epsilon = 3 \times 10^{-7}$ whereas for grazing incidence we gave $\epsilon = 5 \times 10^{-6}$. These do not agree with our present findings. Similar discrepancies were observed with a Cu cathode. In the case of a cathode coated with BaO the efficiency deteriorated rapidly (within 10 laser shots), most probably because, the coating was ablated by the laser pulse. We believe that these problems are related to surface contamination and would be less pronounced at higher fields in the gun.

## 5. Application to a Superconducting r.f. Gun and Piocosecond X-ray Source

Choosing a high microwave frequency allows for a compact structure and cryostat but requires higher fields and better alignment tolerances. So far we have experimented with a 1-1/2 cell copper S-band structure of the Brookhaven design[6] even though an L-band superconducting cavity is contemplated for the actual device.

To accelerate sufficient charge, the electrons, emitted at rest, must reach in the first half cell $\beta = 0.8$ which corresponds to a K.E. gain of 340 keV over a distance of $\lambda/4$. For L-band this requires an average field of only 7 MV/m; this is not difficult to achieve. The Brookhaven S-band cavity is designed for an average field of 66 MV/cm, in which case for a Q-value of $10^8$ the power requirement remains modest

$$P \sim \frac{\lambda^3 \epsilon_0 E^2}{\nu Q} = 7 \text{ W} \tag{6}$$

One can therefore expect higher gradients in the cavity, and we will assume a capture efficiency of 50%.

The electrons will be produced directly at the surface of the cavity at grazing incidence by a 10 ps pulse; this corresponds to a 6° phase angle for the r.f.; synchronization between the laser and r.f. has been achieved. The UV pulse energy will be between 10-100 $\mu$J, and assuming a quantum efficiency $\epsilon = 10^{-5}$ we obtain ~100 pC/pulse in the electron beam. Even though we are presently operating our laser system at 1 Hz, operation at 120 Hz and even at 1 kHz is possible.

For 100 W of input power the gradient in the accelerating structure is 26 MV/m (for $Q = 10^8$, $\nu = 3$ GHz), and the expected energy of the electrons exiting the 1-1/2 cell is 2 MeV. By the addition of two more cells we can reach K.E. = 4.5 MeV. The emittance of the beam is estimated at $(\sigma_x \sigma'_x) \sim 10^{-6}$ m-rad so that one could focus the beam to an area $A = 1$ mm$^2$.

Finally, we consider the backscattering of the main part of the laser pulse from the electron beam. The energy of the backscattered photons is given by $(4\gamma\omega_0/m \ll 1)$

$$\omega = \frac{4\gamma^2\omega_0}{1 + 2\gamma^2(1 - \cos\theta)} \tag{7}$$

where $\gamma = E/m$ for the electron beam, $\omega_0$ is the incident photon energy and $\theta$ is the scattering angle measured from the electron beam direction. Thus for $\theta = 0$

$$\omega = 4\gamma^2\omega_0 \tag{8}$$

Using $\gamma = 10$ and $\omega_0 = 1.16$ eV ($\lambda = 1054$ nm) the backscattered X-rays have a peak energy of 0.46 keV ($\lambda = 26.4$ Å). The energy changes with angle according to Eq. (7), the majority of the spectrum being contained in a forward cone of opening angle $\theta = 1/\gamma \sim 6°$. Thus, by suitable angular collimation a quasi-monochromatic beam can be obtained.

A possible arrangement of the cavity, UV and IR laser ports and X-ray beam line is shown in Fig.7. The yield of X-rays is given by

$$N_x = N_e \frac{N_\omega \sigma_T}{A} \tag{9}$$

where $A$ is the beam area at the interaction point assuming perfect overlap. The total scattering cross section can be approximated by the Thompson value

$$\sigma_T = \frac{8\pi}{3}\, r_0^2 = 6.6 \times 10^{-25}\ \text{cm}^2 \tag{10}$$

We use

$$N_e = 6 \times 10^8 \quad (100\ \text{pC})$$

$$N_\omega = 5 \times 10^{16} \quad (10\ \text{mJ})$$

$$A = 10^{-2}\ \text{cm}^2$$

Therefore $N_x = 2000$/pulse. One can expect an increase in the X-ray yield as the electron beam intensity improves and as the interaction area is further decreased. With existing solid state laser amplifiers a repetition rate of 120 Hz can be reached.

The question arises as to whether the X-rays are coherent. To the extent that the IR laser pulse is coherent one can consider that the X-ray pulse retains this coherence within a particular narrow energy band, primarily in the forward direction. Selecting these forward X-rays one can expect $N_x(\theta) = 200$/pulse. However the principal advantage of the proposed X-ray source is its time resolution and energy tunability, which are achieved by adjusting the laser pulse width and the electron energy, respectively.

Alternately one can let the electron beam traverse a radiator and use the bremsstrahlung as a wide-spectrum, time-resolved $\gamma$-ray source, avoiding the complications of the laser backscattering.

## References and Notes


1. C. Bamber et al., Nuclear Instruments and Methods **A327**, 227 (1993).
2. H. B. Michaelson, J. Appl. Phys. **48**, 4729 (1977).
3. V. S. Fomenko, *Handbook of Thermionic Properties*, ed. by G. V. Samsonov (Plenum Press, New York 1966).
4. J. Fischer and T. Srinivasan-Rao BNL-42151 (1988) Fourth Workshop on Pulse Power Techniques Erice, Italy March 4-9, 1988.
5. V. Peskov, G. Charpak et al., CERN-EP/87-218.
6. K. Batchelor et al., Nuclear Instruments and Methods **A318**, 372 (199?).

## Figure Captions

Fig.1 The laser pulse train used in these experiments.

Fig.2 Schematic of the experimental set-up.

Fig.3 Yield of photoelectrons from a Nb surface in pC/$\mu$J as a function of bias voltage for normal incidence (a) 5mm gap, (b) 1.1 mm gap.

Fig.4 The same data as in Fig.3 as a function of UV energy in the pulse train (a) 5 mm gap (b) 1 mm gap.

Fig.5 Yield of photoelectrons from a Nb surface at grazing incidence for 5.1 mm gap and 3 kV bias a function of laser beam polarization (a) For different UV pulse energies (b) Combined for all energies.

Fig.6 (a) Data from previous experiments for Au, Cu and Nb cathodes (b) Recent data from gold at normal incidence as a function of applied field.

Fig.7 Experimental set-up for proposed X-ray source.

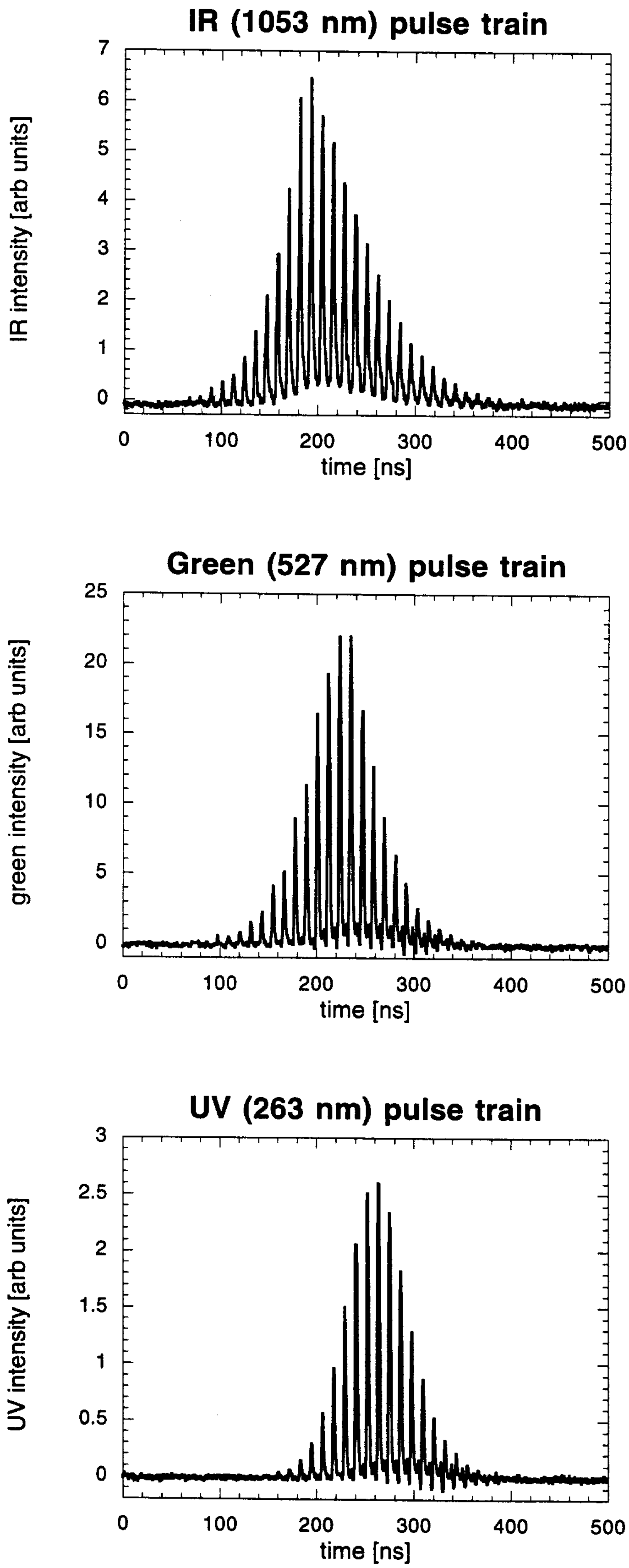
IR (1053 nm) pulse train
IR intensity [arb units]
0
1
2
3
4
5
6
7
0
100
200
300
400
500
time [ns]
Green (527 nm) pulse train
green intensity [arb units]
0
5
10
15
20
25
0
100
200
300
400
500
time [ns]
UV (263 nm) pulse train
UV intensity [arb units]
0
0.5
1
1.5
2
2.5
3
0
100
200
300
400
500
time [ns]

Figure 1

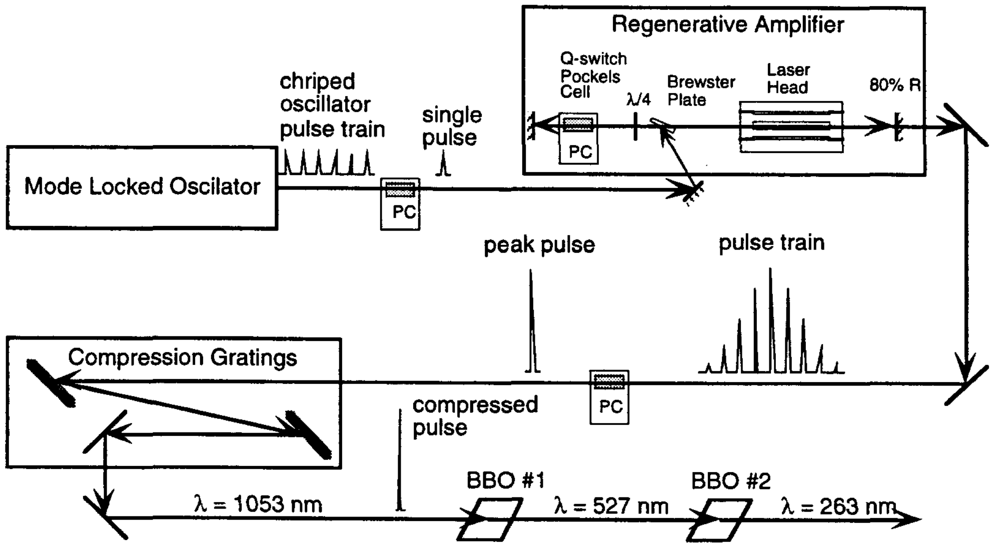
Regenerative Amplifier
Q-switch Pockels Cell
λ/4
Brewster Plate
Laser Head
80% R
chriped oscillator pulse train
single pulse
Mode Locked Oscilator
PC
PC
peak pulse
pulse train
Compression Gratings
PC
compressed pulse
BBO #1
BBO #2
λ = 1053 nm
λ = 527 nm
λ = 263 nm

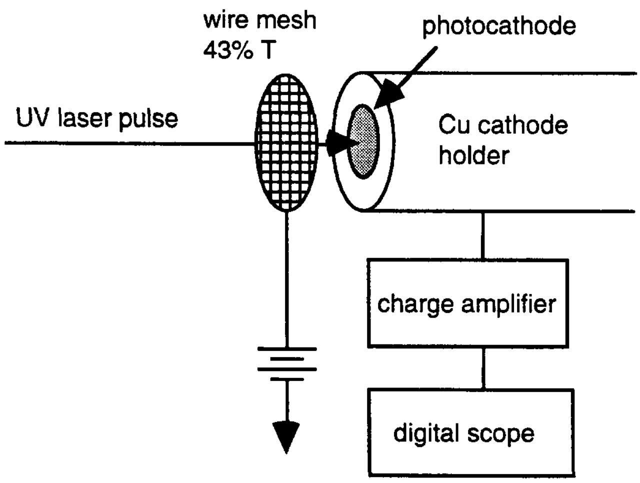
wire mesh
43% T
photocathode
UV laser pulse
Cu cathode holder
charge amplifier
digital scope

Figure 2

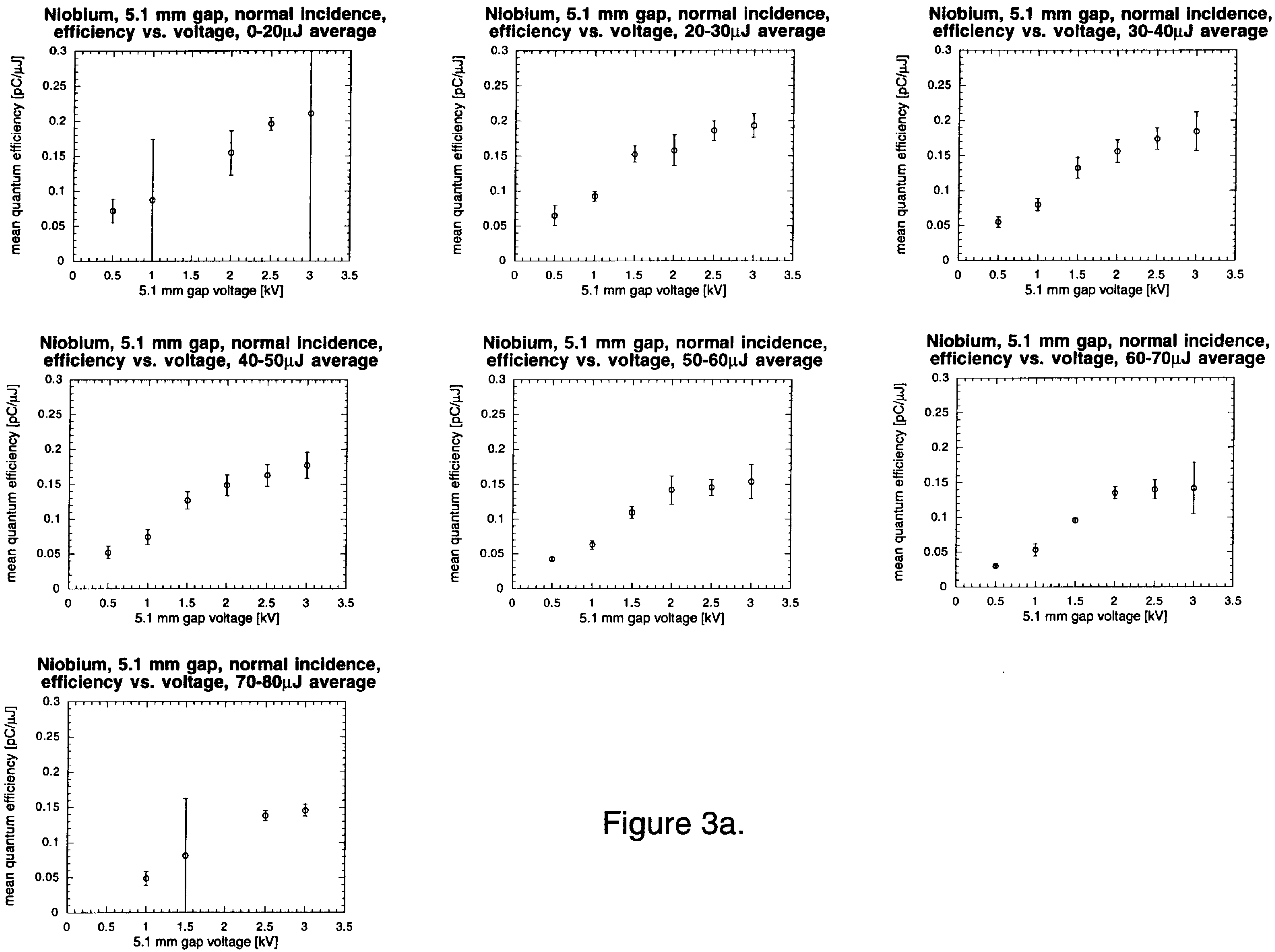
Niobium, 5.1 mm gap, normal incidence, efficiency vs. voltage, 0-20μJ average
Niobium, 5.1 mm gap, normal incidence, efficiency vs. voltage, 20-30μJ average
Niobium, 5.1 mm gap, normal incidence, efficiency vs. voltage, 30-40μJ average
Niobium, 5.1 mm gap, normal incidence, efficiency vs. voltage, 40-50μJ average
Niobium, 5.1 mm gap, normal incidence, efficiency vs. voltage, 50-60μJ average
Niobium, 5.1 mm gap, normal incidence, efficiency vs. voltage, 60-70μJ average
Niobium, 5.1 mm gap, normal incidence, efficiency vs. voltage, 70-80μJ average
mean quantum efficiency [pC/μJ]
5.1 mm gap voltage [kV]
0
0.05
0.1
0.15
0.2
0.25
0.3
0.5
1
1.5
2
2.5
3
3.5

Figure 3a.

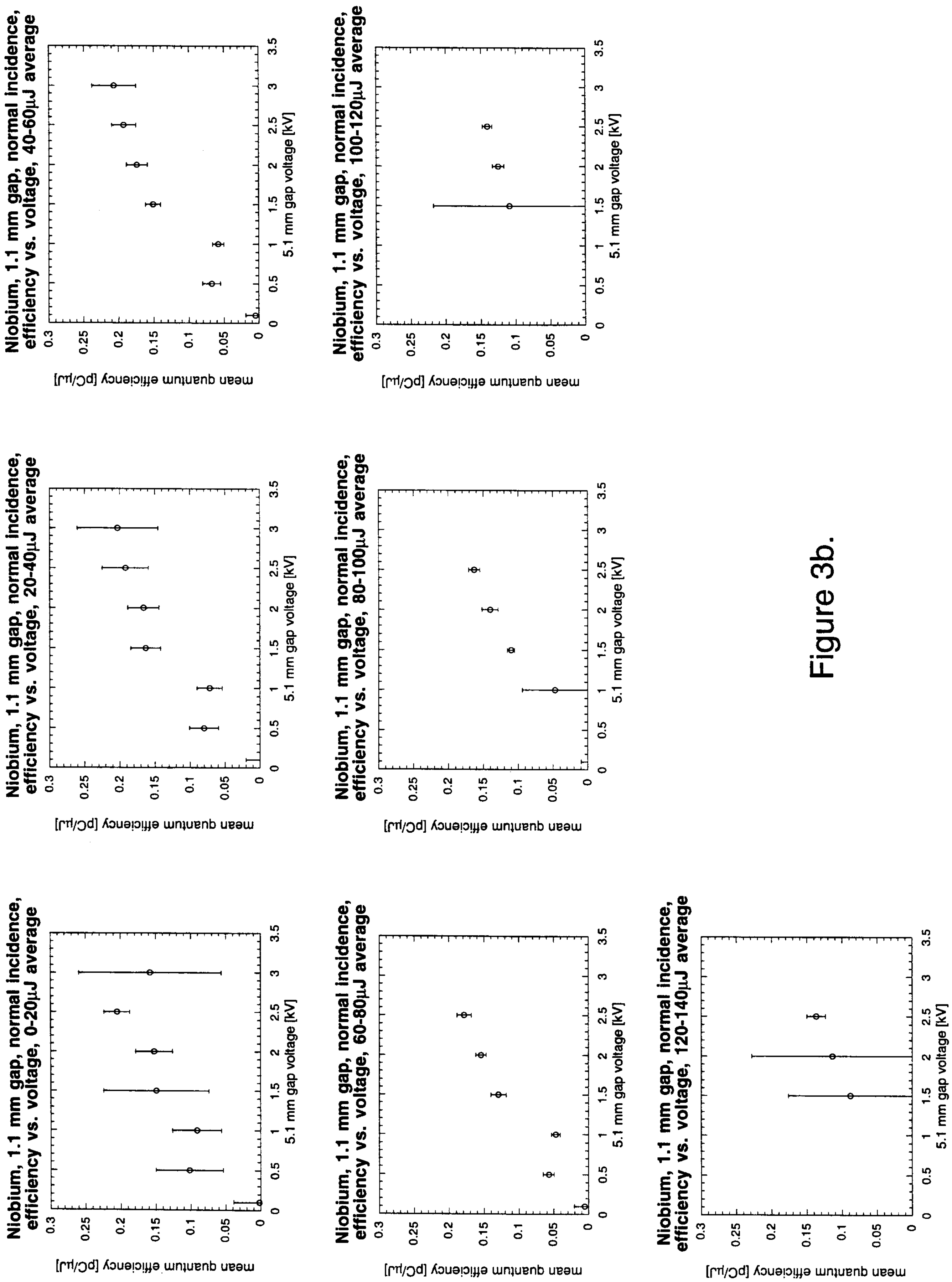
Niobium, 1.1 mm gap, normal incidence, efficiency vs. voltage, 0-20μJ average
Niobium, 1.1 mm gap, normal incidence, efficiency vs. voltage, 20-40μJ average
Niobium, 1.1 mm gap, normal incidence, efficiency vs. voltage, 40-60μJ average
Niobium, 1.1 mm gap, normal incidence, efficiency vs. voltage, 60-80μJ average
Niobium, 1.1 mm gap, normal incidence, efficiency vs. voltage, 80-100μJ average
Niobium, 1.1 mm gap, normal incidence, efficiency vs. voltage, 100-120μJ average
Niobium, 1.1 mm gap, normal incidence, efficiency vs. voltage, 120-140μJ average
mean quantum efficiency [pC/μJ]
5.1 mm gap voltage [kV]
0
0.05
0.1
0.15
0.2
0.25
0.3
0.5
1
1.5
2
2.5
3
3.5

Figure 3b.

Niobium, 1.1 mm gap, normal incidence, quantum efficiency vs. UV energy (20 μJ bin average)

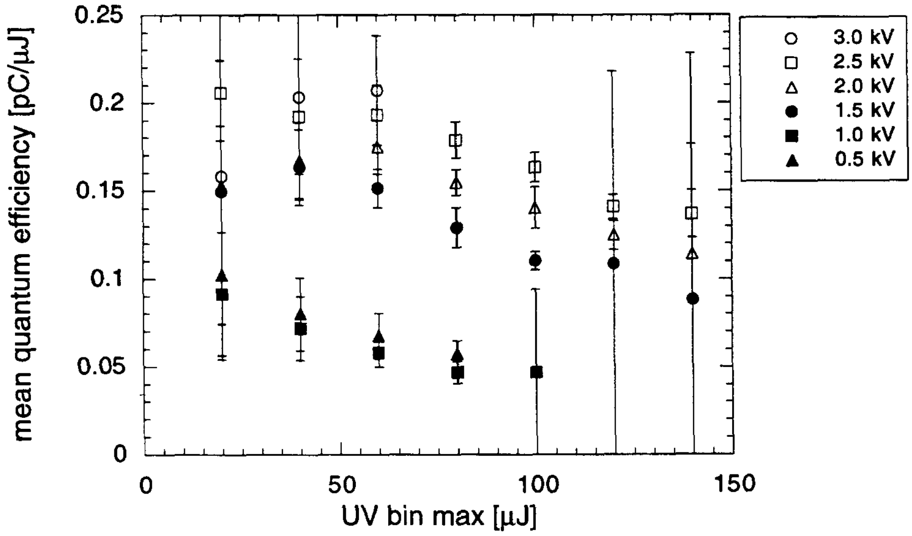


Figure 4a

Niobium, 5.1 mm gap, normal incidence, quantum efficiency vs. UV energy (10 μJ bin average)

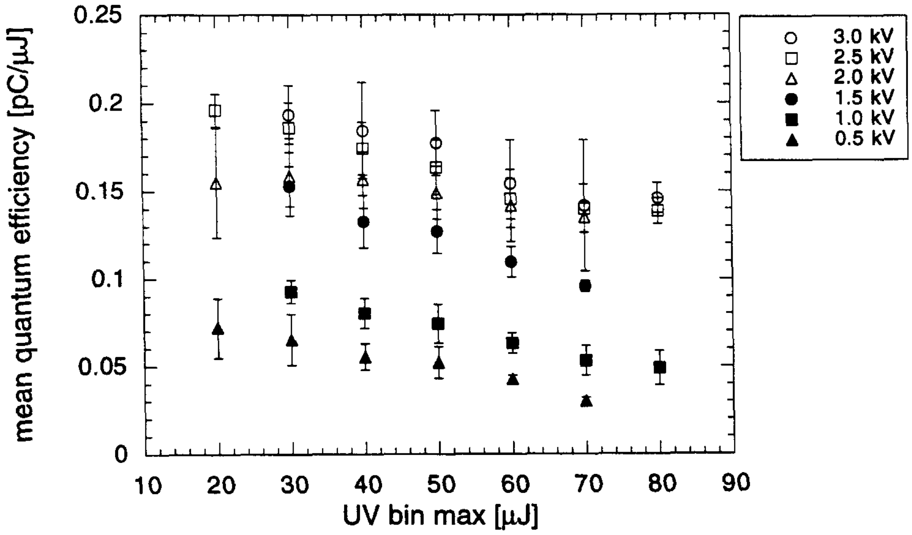


Figure 4b

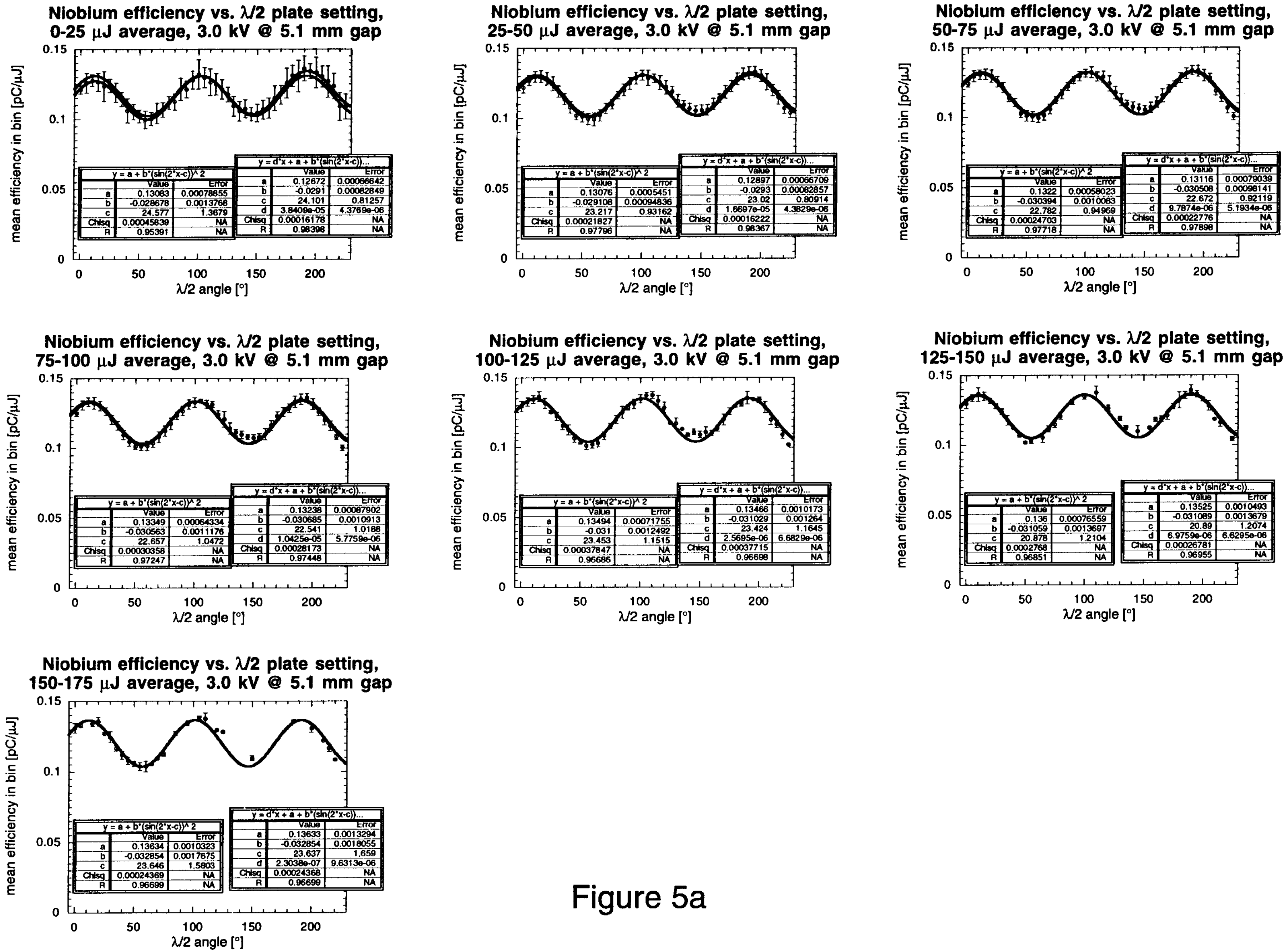
Niobium efficiency vs. λ/2 plate setting, 0-25 μJ average, 3.0 kV @ 5.1 mm gap
mean efficiency in bin [pC/μJ]
λ/2 angle [°]
y = a + b*(sin(2*x-c))^2
a 0.13083 0.00078655
b -0.028678 0.0013768
c 24.577 1.3679
Chisq 0.00045839 NA
R 0.95391 NA
y = d*x + a + b*(sin(2*x-c))...
a 0.12672 0.00066642
b -0.0291 0.00082849
c 24.101 0.81257
d 3.8409e-05 4.3769e-06
Chisq 0.00016178 NA
R 0.98398 NA
Niobium efficiency vs. λ/2 plate setting, 25-50 μJ average, 3.0 kV @ 5.1 mm gap
y = a + b*(sin(2*x-c))^2
a 0.13076 0.0005451
b -0.029108 0.00094836
c 23.217 0.93162
Chisq 0.00021827 NA
R 0.97796 NA
y = d*x + a + b*(sin(2*x-c))...
a 0.12897 0.00056709
b -0.0293 0.00082857
c 23.02 0.80914
d 1.6697e-05 4.3829e-06
Chisq 0.00016222 NA
R 0.98367 NA
Niobium efficiency vs. λ/2 plate setting, 50-75 μJ average, 3.0 kV @ 5.1 mm gap
y = a + b*(sin(2*x-c))^2
a 0.1322 0.00058023
b -0.030394 0.0010063
c 22.782 0.94969
Chisq 0.00024703 NA
R 0.97718 NA
y = d*x + a + b*(sin(2*x-c))...
a 0.13116 0.00079039
b -0.030508 0.00098141
c 22.672 0.92119
d 9.7874e-06 5.1934e-06
Chisq 0.00022776 NA
R 0.97898 NA
Niobium efficiency vs. λ/2 plate setting, 75-100 μJ average, 3.0 kV @ 5.1 mm gap
y = a + b*(sin(2*x-c))^2
a 0.13349 0.00064334
b -0.030563 0.0011176
c 22.657 1.0472
Chisq 0.00030358 NA
R 0.97247 NA
y = d*x + a + b*(sin(2*x-c))...
a 0.13238 0.00087902
b -0.030685 0.0010913
c 22.541 1.0188
d 1.0425e-05 5.7759e-06
Chisq 0.00028173 NA
R 0.97448 NA
Niobium efficiency vs. λ/2 plate setting, 100-125 μJ average, 3.0 kV @ 5.1 mm gap
y = a + b*(sin(2*x-c))^2
a 0.13494 0.00071755
b -0.031 0.0012492
c 23.453 1.1515
Chisq 0.00037847 NA
R 0.96686 NA
y = d*x + a + b*(sin(2*x-c))...
a 0.13466 0.0010173
b -0.031029 0.001264
c 23.424 1.1645
d 2.5695e-06 6.6829e-06
Chisq 0.00037715 NA
R 0.96698 NA
Niobium efficiency vs. λ/2 plate setting, 125-150 μJ average, 3.0 kV @ 5.1 mm gap
y = a + b*(sin(2*x-c))^2
a 0.136 0.00076559
b -0.031059 0.0013697
c 20.878 1.2104
Chisq 0.0002768 NA
R 0.96851 NA
y = d*x + a + b*(sin(2*x-c))...
a 0.13525 0.0010493
b -0.031089 0.0013679
c 20.89 1.2074
d 6.9759e-06 6.6295e-06
Chisq 0.00026781 NA
R 0.96955 NA
Niobium efficiency vs. λ/2 plate setting, 150-175 μJ average, 3.0 kV @ 5.1 mm gap
y = a + b*(sin(2*x-c))^2
a 0.13634 0.0010323
b -0.032854 0.0017675
c 23.646 1.5803
Chisq 0.00024369 NA
R 0.96699 NA
y = d*x + a + b*(sin(2*x-c))...
a 0.13633 0.0013294
b -0.032854 0.0018055
c 23.637 1.659
d 2.3038e-07 9.6313e-06
Chisq 0.00024368 NA
R 0.96699 NA

Figure 5a

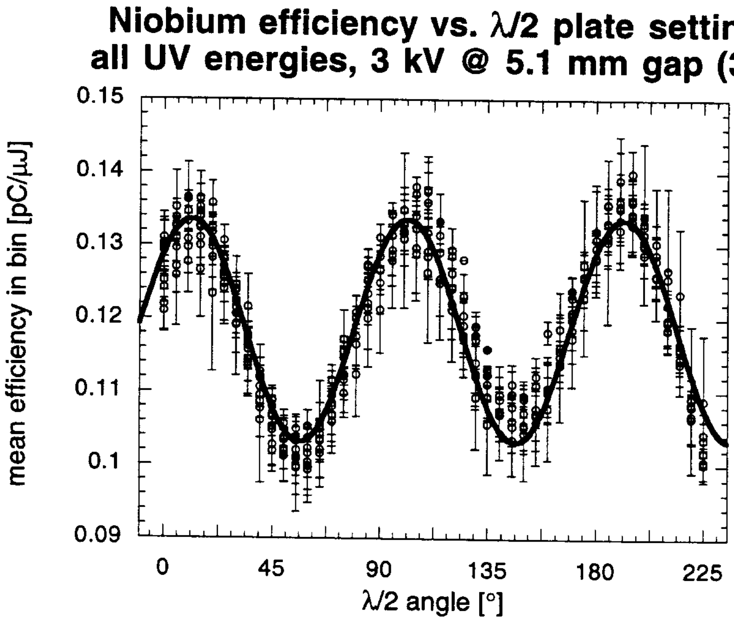


| y = a + b*(sin(2*x-c))^2 | | |
|---|---|---|
| | Value | Error |
| a | 0.13353 | 0.0002885 |
| b | -0.03044 | 0.000503 |
| c | 23.285 | 0.47222 |
| Chisq | 0.0033836 | NA |
| R | 0.95784 | NA |

Figure 5b

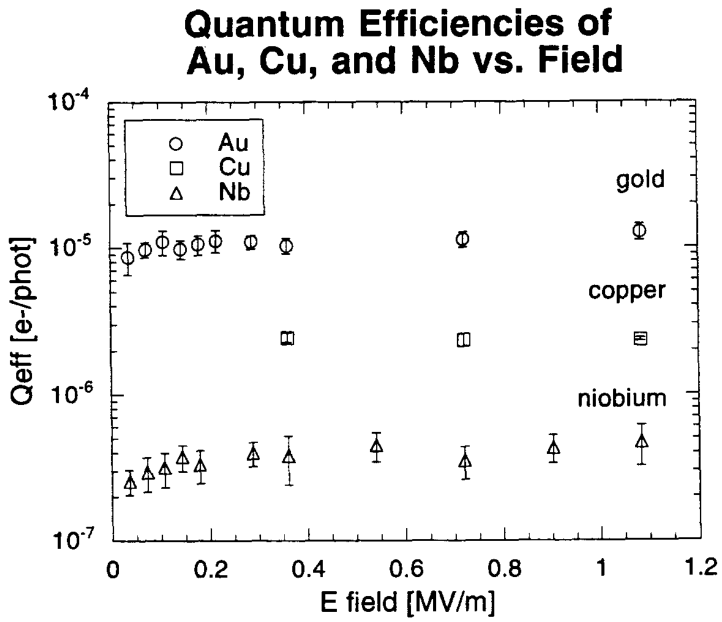


Figure 6a

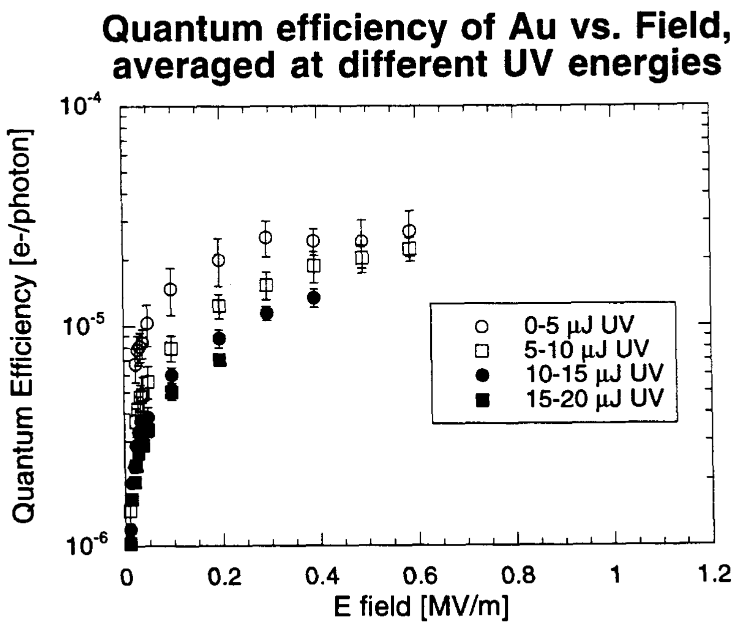


Figure 6b

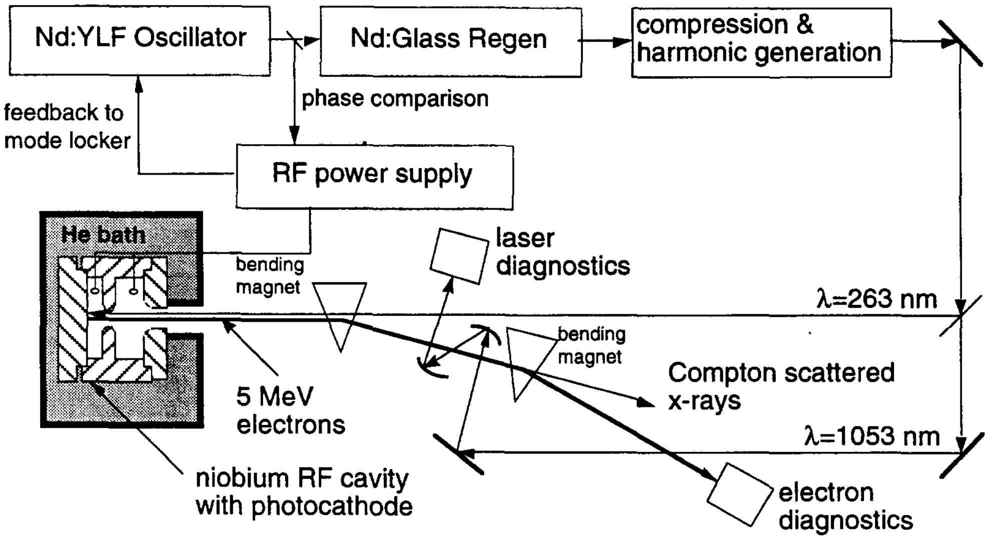
Nd:YLF Oscillator
Nd:Glass Regen
compression &
harmonic generation
feedback to
mode locker
phase comparison
RF power supply
He bath
bending
magnet
laser
diagnostics
λ=263 nm
bending
magnet
Compton scattered
x-rays
5 MeV
electrons
λ=1053 nm
niobium RF cavity
with photocathode
electron
diagnostics

Figure 7